

A Generative Adversarial Network Approach to Metastatic Cancer Cell Images

Seohyun Lee¹, Hyuno Kim², Hideo Higuchi³, Masatoshi Ishikawa⁴, and Ryuichiro Natato¹

¹Laboratory of Computational Genomics, Institute for Quantitative Bioscience, The University of Tokyo
1-1-1 Yayoi, Bunkyo-ku, Tokyo, Japan

²Department of Mechanical and Biofunctional Systems, Institute of Industrial Science, The University of Tokyo
4-6-1 Komaba, Meguro-ku, Tokyo, Japan

³Department of Physics, Graduate School of Science, The University of Tokyo

⁴Data Science Research Division, Information Technology Center, The University of Tokyo
7-3-1 Hongo, Bunkyo-ku, Tokyo, Japan

seohyun_lee@iqb.u-tokyo.ac.jp

h-kim@iis.u-tokyo.ac.jp

higuchi@phys.s.u-tokyo.ac.jp

ishikawa@ishikawa-vision.org

rnatato@iqb.u-tokyo.ac.jp

Abstract—The shapes of metastatic cancer cells are considered to be relatively different from non-metastatic cancer cells, especially regarding the degree of development of lamellipodia or the pattern of internal organ arrangement. However, understanding the specific pattern of the metastatic cancer cell has just started to emerge. In this paper, based on the generative adversarial network approach, we attempted to generate metastatic cancer cell images using human breast cancer cells where the metastasis-promoting protein, PAR1, is expressed.

Index Terms—generative adversarial network, cell image classification, breast cancer cell, biomedical image analysis, deep learning.

I. INTRODUCTION

Cancer indicates the phenomenon that the cells do not follow the apoptotic pathway but grow uncontrollably [1]. Although the possibility of staying as a benign tumor is still high if the cells remain at their original position, it is considered malignant when the cells spread from the primary location to the other parts of the body [2]. The process of this dissemination is known as tumor metastasis, which makes cancer the most deadly disease with high morbidity rates [3]–[5].

Therefore, there have been many studies to understand the internal signal pathway in the cancer cell and to develop medical treatments using the knowledge of the nanoscale movement of intracellular information carrier, because the uncontrolled cell signal cascade is considered to be one of the essential key factors for the cancer research [1], [2].

Regarding intracellular dynamics, a huge amount of studies have been conducted to elucidate the specific mechanism of information delivery. Particularly, the three-dimensional movement of vesicles in terms of the interaction with the cytoskeletons such as actin filament and microtubule was interpreted based on numerical analysis, [6], [7] with the report

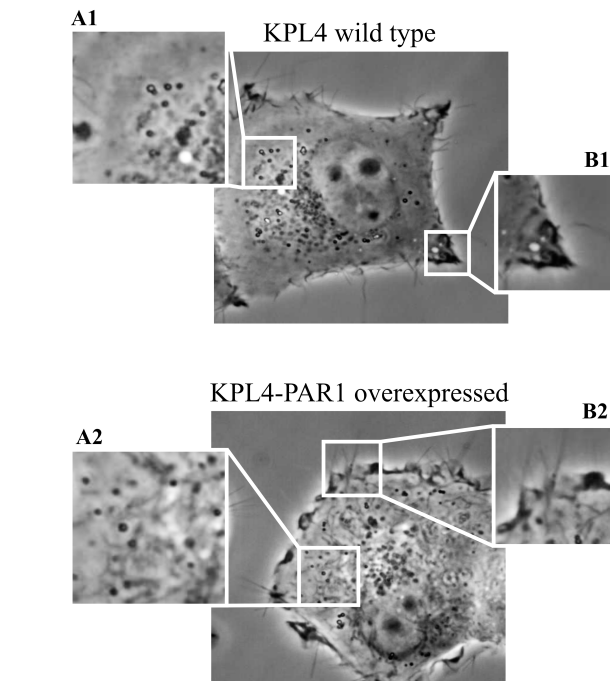
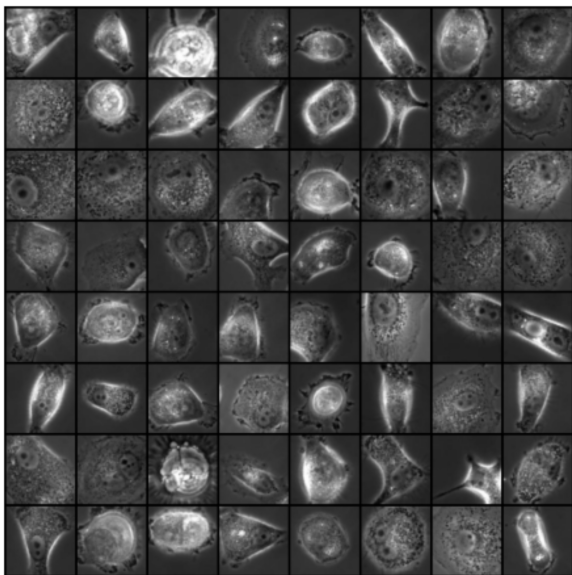


Fig. 1. Recognizable difference in cell morphology between representative KPL4 wild type which is relatively non-metastatic (upper) and protease-activated receptor 1 (PAR1) overexpressing KPL4 cancer cell which is considered highly metastatic (lower). A1 and A2 show the pattern of vesicle distribution while B1 and B2 indicate the difference in the development of filopodia and lamellipodia, and the contour profile of the cell.

about the characteristic rotational movement of cargoes on the cytoskeletal networks [8], [9]. Additionally, recent studies also attempted to introduce machine learning and image processing method based on computer vision into the cellular dynamics of the information carriers of interest [10]–[12].

A.

Training Images of KPL4-PAR1 overexpressed cell



B.

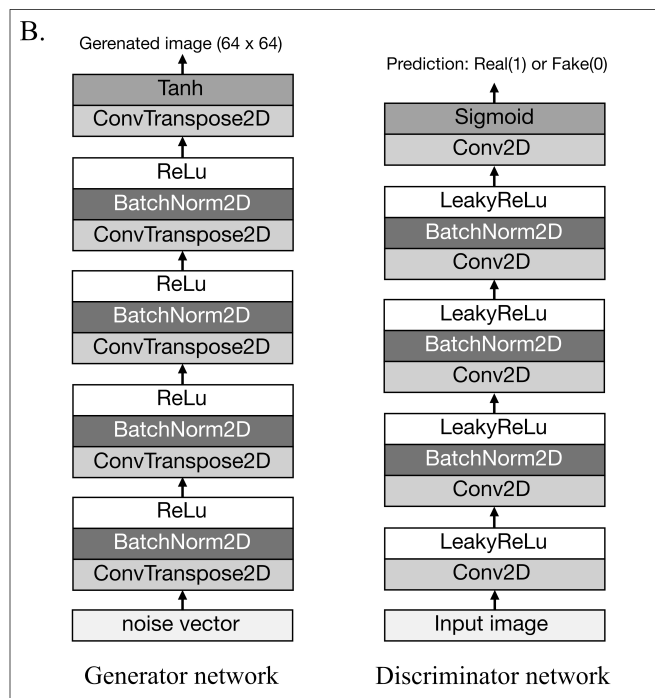


Fig. 2. (A) A representative training dataset of KPL4-PAR1 overexpressed cancer cell images. (B) The structures of the generator network and the discriminator network exploited in this study.

The studies introduced above shed light on our understanding of the practical movement of the signal carriers in the cancer cell, but the process of metastasis, which is in charge of leading cancer to lethal disease, has not yet been fully elucidated. Recently, because there have been studies to identify the mutation of a specific protein that promotes the mobility of metastatic cancer cells, many researchers have started to focus on the morphology of the cancer cell, as the irregular shape of the cancer cell is frequently accompanied by the enhanced mobility for the higher rate of cell migration [13].

For example, as shown in Fig. 1, the shape of the metastatic cancer cell can differ from relatively non-metastatic cancer cells, in the case of the KPL4 human breast cancer cell. Human observers can detect the different characteristics in morphology between two different cell types, such as the distribution pattern of internal organs (A1 and A2) and the development of filopodia and lamellipodia as well as the contour profile of the cell (B1 and B2). Therefore, recent studies have started to focus on big data of metastatic cancer cell images to develop deep-learning algorithms for the classification mainly using such differences in tissue-level morphology [14]–[16]. In our previous study, we suggested a deep-learning approach to classifying the type of KPL4 cancer cell, only using their phase-contrast microscopy images of colony morphology.

In this study, we attempted to introduce a generative adversarial network (GAN) approach [17] into the mimicry of the morphology of metastatic cancer cells, in order to augment the cell shape dataset for a more refined classification task [18].

II. DATA PREPARATION

A. Live Cell Imaging

The KPL4 human breast cancer cell line was kindly provided by Dr. Kurebayashi [19] (Kawasaki Medical School, Kurashiki, Japan). The cells exploited for the imaging were cultured in a complete growth medium (Dulbecco’s modified Eagle’s medium with high glucose, Nacalai Tesque, Inc., Japan) and then incubated at 37°C with 5% of CO₂. During the imaging experiment, cells were stored in the heater (IN-ONI-F1, Tokai HIT, Shizuoka, Japan) to maintain the physiological conditions of living cells.

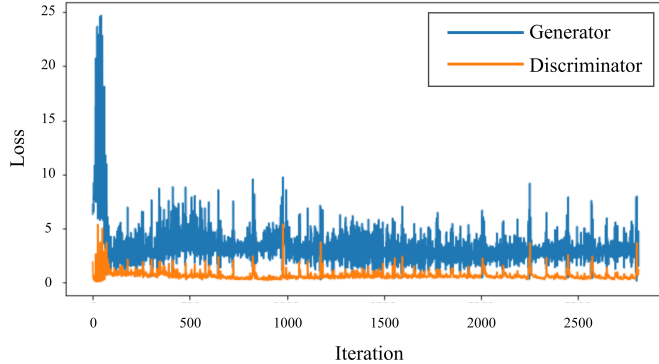
The images of the individual KPL4-PAR1 overexpressed cancer cells were taken by CMOS camera (Andor, DG-152X-C0E-F1, Belfast, Northern Ireland) with the microscope (IX70, Olympus, Tokyo, Japan) where 60× of objective lens is installed with a stage stabilizer [20]. In order to obtain clearly defined images of the intracellular area as well as cell edges, the phase-contrast imaging method, which enhances the contrast based on optical technique, was exploited in the imaging experiment. The size of raw images was 500×500.

B. Data Preprocessing and Augmentation

Followings are the process to prepare the KPL4-PAR1 overexpressed cancer cell image dataset as shown in Fig. 2(A). First of all, the size of all the raw images was reduced to 200×200 to lower computational cost. Second, since the initial number of prepared images was only 360, the dataset was augmented by rotating and cropping the images. Because the size of the image after the transformation basically decreases

A.

Loss of Generator and Discriminator during Training



B. Fake images generated at n th iteration

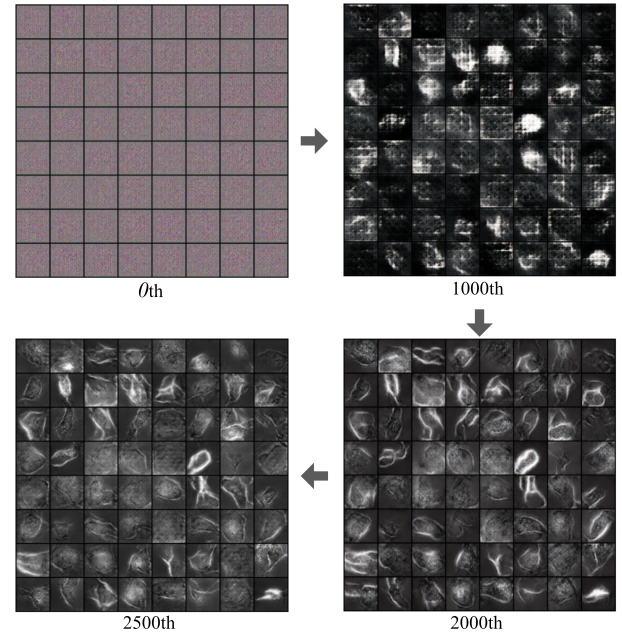


Fig. 3. (A) Loss of generator and discriminator during training. (B) A series of fake images created by generator network at 0th, 1000th, 2000th, and 2500th iteration.

as the rotation angle increases, we set the incremental angle as 0.1 degrees, and the initial angle as $n\pi/2$ ($n=1, 2, 3, 4$). The rotation was conducted for 5 degrees in maximum ($0 < \theta < 5$). After the rotation, the images were cropped to generate the largest possible square using the image crop function in Python Image Library. The four arguments for the crop, which determine the left, upper, right, and lower positions, respectively, were calculated as below.

$$(\text{left, upper, right, lower}) = (\alpha, \alpha, s - \alpha, s - \alpha) \quad (1)$$

where s indicates the size of expanded image produced by the rotation of the original image and α refers to the value computed by the following calculation in the case of the rotation by θ .

$$\alpha = s \times (\sin \theta \times \cos \theta / (\sin \theta + \cos \theta)) \quad (2)$$

Utilizing the above data augmentation method, the volume of the total image dataset was enlarged to 72,000 and the images were fed to the generator as well as discriminator models with the batch size 128.

III. MODEL CONSTRUCTION

A. Experimental Condition

In the experiment, the models were constructed by using the Pytorch framework (version 0.4.1) with Python version 3.7.9, in Linux (Ubuntu 16.04 LTS) operating system. The number of epoch for the training was set to 5, which produces

approximately 2,800 iterations with a batch size of 128 for 72,000 images in total. Additionally, the loss was computed using Binary Cross-Entropy loss, and Adam optimizer [22] was exploited for both generator and discriminator networks.

B. Deep Convolutional Generative Adversarial Network

The practical structure for the cancer cell image generator and discriminator networks were constructed based on the deep convolutional generative adversarial network (DCGAN), one of the extended GAN, which respectively utilizes convolutional and convolutional-transpose layers for the discriminator and the generator network [21]. Composed of convolutional-transpose layers, batch normalization layers, and ReLU activation, the generator network produces fake images from a noise vector in order to deceive the discriminator. On the other hand, the discriminator network comprises convolution layers, batch normalization layers, and LeakyReLU activation to discern the real images from fake images created by the generator network. The entire structures of the generator and discriminator are as shown in Fig. 2(B).

IV. RESULT AND DISCUSSION

The loss over iteration for generator and discriminator network is as shown in Fig. 3(A) and the fake images created by generator network at 0th, 1000th, 2000th, and 2500th iterations are as shown in Fig. 3(B). The generator loss was computed by $\log D(G(z))$ where z indicates the latent vector and G represents the generator network which outputs the image while D refers to the discriminator network which produces a

scalar probability that $G(z)$ is real. Likewise, discriminator loss is calculated as $\log D(x) + \log(1 - D(G(z)))$ where $D(x)$ means the average output for all the real batches by the discriminator, which is the sum of the losses for the real and fake batches. The goal of GAN is achieved when the generator can produce perfect fake images so that the discriminator can guess with 50% of confidence. In this experiment, the fake images were stably created when the iteration reaches approximately 2000, as shown in Fig. 3(A), and the level of loss lingers until the final epoch. Accordingly, the quality of fake images produced by the generator network remains similar when iteration is over approximately 2000, as shown in Fig. 3(B).

Although the generator loss was reduced overall and the value of $D(G(z))$ oscillates between 0.1 and 0.6, the goal of which is 0.5, the generated cell images are still recognizable as fake by human observers. First, the generator network is good at defining the edges of cells, but the location of the nucleus and the distribution of internals still seems obscure in the produced images. In addition, as the loss of the generator network did not apparently decrease after the 2000th iteration, the quality of generated cell images was not seemingly enhanced.

Because the main reason we attempted to produce fake cancer cell images is to augment the image dataset which can be subjected to the classification task for distinguishing metastatic and non-metastatic cancer cell lines only by their images, optimization of the number of epochs as well as the structural composition of both generator and discriminator are remained to be improved in the future work. Moreover, not only the KPL4-PAR1 overexpressed cell line but also the KPL4 wild type cell line which is known to be relatively less metastatic should be included in the next experiment, in order to prepare similar amounts of the image dataset. If we are able to compose and train the image dataset made of DCGAN-based augmentation besides real microscopy images for KPL4-PAR1 overexpressed cell and KPL4 wild type cell, it is expected to help our understanding of the morphological characteristics of metastatic cancer cell lines.

V. CONCLUSION

In this paper, the microscopy images of the KPL4-PAR1 overexpressed cell line, which is known to be a metastatic human breast cancer cell, were generated by DCGAN. The raw cell images were obtained by using phase-contrast microscopy, and the volume of the dataset was enlarged based on the rotation and cropping of the images. After the 2000th iteration, the generator network was able to produce the images that discriminator can tell the genuineness of the images by approximately between 0.1 to 0.6, and a human observer can detect the similar shapes of cell edges compared to real cell images. With more improvement in layer composition and image data preparation, the result shown in this study is expected to be exploited in data augmentation for metastatic cancer cell classification task, which aims to understand the individual morphology of highly metastatic cancer cell lines.

REFERENCES

- [1] R. J. Bold, P. M. Termuhlen, and D. J. McConkey, "Apoptosis, cancer and cancer therapy," *Surgical oncology*, 6(3), pp. 133–142. 1997.
- [2] H. Chen, W. Zhang, G. Zhu, J. Xie, and X. Chen, "Rethinking cancer nanotheranostics," *Nature Reviews Materials*, 2(7), pp. 1–18. 2017.
- [3] Petersen, "Oral cancer prevention and control—the approach of the World Health Organization," *Oral oncology*, 45(4-5), pp. 454–460. 2009.
- [4] F. Bray, J. Ferlay, I. Soerjomataram, R. L. Siegel, L. A. Torre, and A. Jemal, "Global cancer statistics 2018: GLOBOCAN estimates of incidence and mortality worldwide for 36 cancers in 185 countries," *CA: a cancer journal for clinicians*, 68(6), pp. 394–424. 2018.
- [5] B. Weigelt, J. L. Peterse, and L. J. Van't Veer, "Breast cancer metastasis: markers and models," *Nature reviews cancer*, 5(8), pp. 591–602. 2005.
- [6] S. Lee, H. Kim, and H. Higuchi, "Numerical method for vesicle movement analysis in a complex cytoskeleton network," *Optics express*, 26(13), pp. 16236–16249. 2018.
- [7] S. Lee, H. Kim, and H. Higuchi, "Extended dual-focus microscopy for ratiometric-based 3D movement tracking," *Applied Sciences*, 10(18), 6243.
- [8] J. P. Bergman, M. J. Bovyn, F. F. Doval, A. Sharma, M. V. Gudheti, S. P. Gross, J. F. Allard, and M. D. Vershinin, "Cargo navigation across 3D microtubule intersections," *Proceedings of the National Academy of Sciences*, 115(3), pp. 537–542. 2018.
- [9] S. Lee and H. Higuchi, "3D rotational motion of an endocytic vesicle on a complex microtubule network in a living cell," *Biomedical Optics Express*, 10(12), pp. 6611–6624. 2019.
- [10] S. Lee, H. Kim, M. Ishikawa, and H. Higuchi, "3D Nanoscale tracking data analysis for intracellular organelle movement using machine learning approach," In *Proc. IEEE Int. Conf. Artificial Intelligence in Information and Communication*, pp. 181–184. 2019.
- [11] S. Lee, H. Kim, H. Higuchi, and M. Ishikawa, "Visualization and data analysis for intracellular transport using computer vision techniques," In *Proc. IEEE Sensors Applications Symposium*, pp. 1–6. 2020.
- [12] S. Lee, H. Kim, H. Higuchi, and M. Ishikawa, "Visualization method for the cell-level vesicle transport using optical flow and a diverging colormap," *Sensors*, 21(2), pp. 1–13. 2021.
- [13] T. Lv, X. Wu, L. Sun, Q. Hu, Y. Wan, L. Wang, Z. Zhao, Z. Tu, and Z. X. J. Xiao, "p53-R273H upregulates neuropilin-2 to promote cell mobility and tumor metastasis," *Cell death & disease*, 8(8), pp. e2995–e2995. 2017.
- [14] D. Wang, A. Khosla, R. Gargeya, H. Irshad, and A. H. Beck, "Deep learning for identifying metastatic breast cancer," *arXiv preprint arXiv:1606.05718*. 2016.
- [15] B. E. Bejnordi, M. Veta, P. J. Van Diest, B. Van Ginneken, N. Karssemeijer, G. Litjens, J. A. W. M. van der Laak, and O. Geessink, "Diagnostic assessment of deep learning algorithms for detection of lymph node metastases in women with breast cancer," *Jama*, 318(22), pp. 2199–2210. 2017.
- [16] W. Jiao, G. Atwal, P. Polak, R. Karlic, E. Cuppen, A. Danyi, J. de Ridder, C. van Herpen, M. P. Lolkema, N. Steeghs, G. Getz, Q. Morris and L. D. Stein, "A deep learning system accurately classifies primary and metastatic cancers using passenger mutation patterns," *Nature communications*, 11(1), pp. 1–12. 2020.
- [17] I. Goodfellow, J. Pouget-Abadie, M. Mirza, B. Xu, D. Warde-Farley, S. Ozair, A. Courville, and Y. Bengio, "Generative adversarial nets," *Advances in neural information processing systems*, 27, 2014.
- [18] S. Lee, H. Kim, H. Higuchi, M. Ishikawa, "Classification of Metastatic Breast Cancer Cell using Deep Learning Approach," In *Proc. IEEE Int. Conf. Artificial Intelligence in Information and Communication*, pp. 425–428. 2021.
- [19] J. Kurebayashi, T. Otsuki, C. K. Tang, M. Kurosumi, S. Yamamoto, K. Tanaka, M. Mochizuki, H. Nakamura, and H. Soono, "Isolation and characterization of a new human breast cancer cell line, KPL-4, expressing the Erb B family receptors and interleukin-6," *British journal of cancer*, 79(5), pp. 707–717. 1999.
- [20] S. Lee, H. Kim, and H. Higuchi, "Focus stabilization by axial position feedback in biomedical imaging microscopy," In *Proc. IEEE Sensors Applications Symposium*, pp. 1–6. 2018.
- [21] A. Radford, L. Metz, and S. Chintala, "Unsupervised representation learning with deep convolutional generative adversarial networks," *arXiv preprint arXiv:1511.06434*. 2015.
- [22] D. P. Kingma and J. Ba, "Adam: A method for stochastic optimization," *arXiv preprint arXiv:1412.6980*, 2014.